ELSEVIER

Agricultural Systems, Vol. 51, No. 4, pp. 377–393, 1996

0308-521X/96 $15.00 + .00

0308-521X(95)00068-2

Modelling Diurnal Patterns of Air Temperature, Radiation Wind Speed and Relative Humidity by Equations from Daily Characteristics

J. E. Ephrath,[a] J. Goudriaan[b] & A. Marani[c]

[a]Ben-Gurion University of the Negev, The Jacob Blaustein Institute for Desert Research, The Albert Katz Center for Desert Agrobiology, Sede-Boqer 84993, Israel
[b]Agricultural University, Department of Theoretical Production Ecology, P.O. Box 430, 6708 AK, Wageningen, The Netherlands
[c]Hebrew University of Jerusalem, Faculty of Agriculture, P.O. Box 12, Rehovot 76100, Israel

(Received 19 June 1995; accepted 12 November 1995)

ABSTRACT

Calculated data on diurnal patterns from daily averages can be useful as inputs for models simulating plant processes such as photosynthesis and transpiration. A method was developed for the calculation of diurnal patterns of air temperature, wind speed, global radiation and relative humidity from available daily data. Calculated data were validated with measured data collected in Israel, California and The Netherlands. A simple sine-exponential method for describing diurnal air temperature was not sufficient in most cases, and the addition of parameters which specified the time lag of maximum temperature and the effect of buoyancy improved the data accuracy. Diurnal course of wind speed could be described using two sine curves scaled by the measured daily total wind run. Time base of each of the sine curves and the minimum wind speed had to be defined for each location. An accurate description of the diurnal global radiation was obtained, based on the measured daily total global radiation, and the calculated sine of the solar elevation corrected for atmospheric transmissivity. Relative humidity was calculated from the dew point temperature computed as the minimum value of a characteristic seasonal value or the actual air temperature. When the site-specific parameters were known or correctly estimated these methods gave good estimations of the diurnal weather patterns. Copyright © 1996 Elsevier Science Ltd

NOMENCLATURE

AMP	Amplitude of the T_{min} and T_{max} temperature °K
C	Meteorological characteristic defining dependence of transmissivity on solar height –
CD	The amplitude of the sine of the solar height –
DL	Day length h
DSBE	The daily total of the effective solar height –
e_s	Saturated vapour pressure in the air kPa
J	Index of the day –
L	Latitude degree
LSH	The time of maximum solar height h
P	The delay in air T_{max} with respect to LSH h
$R_{g(a)}$	Current global radiation intensity W m^{-2}
$R_{g(tot)}$	Daily total global radiation J m^{-2}
RH	Relative humidity %
$S_{(t)}$	Dimensionless function of time –
SD	The seasonal offset of the sine of the solar height –
$SF_{1,2}$	Time duration factors for wind speed h
$\sin\beta$	The sine of the solar elevation –
t_a	Current time h
T_a	Current air temperature °C
T_d	Dew point temperature °C
$T_{d(cal)}$	Calculated dew point temperature °C
$T_{d(max)}$	Assumed maximum dew point temperature °K
$tw_{1,2}$	Timing factors for wind speed h
T_k	A parameter which specified the effect of buoyancy °K
T_{max}	Maximum daily air temperature °C
T_{min}	Minimum daily air temperature °C
t_s	Sunset time h
T_s	Sunset temperature °C
TOT_w	Daily total wind run km d^{-1}
VPA	Actual vapour pressure in the air kPa
W_a	Current wind speed m s^{-1}
W_{max}	Maximum wind speed m s^{-1}
W_{min}	Minimum wind speed m s^{-1}
δ	Solar declination degree
η	Night length ($\eta = 24$–DL) h
τ	Time coefficient h

INTRODUCTION

Temperature, radiation and other weather variables obviously have a very important effect on many physiological processes taking place in plants. Most of these data are usually available as daily totals (wind speed and radiation) or daily maximums and minimums (temperature and relative humidity).

Daily totals or daily averages are convenient to work with and usually offer a good representation of the average climate. Daily totals may be sufficient in some situations. For instance, when the development rate of plants is proportional to temperature, reckoned from a base temperature, the day degrees or the heat units methods (Wang, 1960; Bernhardt & Shepard, 1978) can be calculated from average daily temperatures. In estimating crop responses, however, the use of daily weather values causes deviations. Most physiological processes, such as photosynthesis (Björkman, 1979), enzymatic activity, respiration, transpiration, translocation and absorption of nutrients, respond instantaneously to weather variables, so that daily totals or means of the required weather data are not sufficient. Deviations are particularly caused by non-linear reactions, such as the response of photosynthesis to light which is saturated at high light intensities, or the non-linear temperature response of some processes, the rate of which can be adversely affected by high temperatures.

A second type of deviation is caused by the interaction of different climatic factors. For example, transpiration rate is affected by wind speed as well as by radiation intensity and relative humidity. This interaction is a potential source of errors when the Penman (1948) equation is computed on the basis of daily weather data.

These considerations have stimulated the development of computer techniques, whereby diurnal curves calculated from daily data can be used as inputs for simulating crop growth rate and its development (Geng *et al.*, 1985). Several authors suggested ways to describe the diurnal temperature curve from minimum and maximum data (Richardson, 1981, 1982; Floyd & Braddock, 1984).

The purpose of the work presented here is to investigate the feasibility of deriving the diurnal curves of air temperature, global radiation, wind speed and relative humidity, from daily data collected by standard meteorological methods.

MATERIALS AND METHODS

Measurements in Israel

Standard climatic data were collected (from May to September 1986 and from April to July 1987) at 15 min intervals in the coastal plain of

Israel (latitude 32°) from a meteorological station connected to a CR-21X data-logger (Campbell Sci. Co., Logan, UT, USA).

Air temperature was measured at the height of 2 m using a copper–constantan thermocouple. Thermocouples were placed in a shaded and ventilated chamber to prevent direct solar-radiation from influencing the readings. Wind speed was measured at the same height using a three-cup anemometer (model 12102; R. M. Young Co., USA). Global radiation was measured using a solarimeter (model CM5; Kipp & Zonen, Delft, The Netherlands). Relative humidity data was measured from the beginning of August 1987 using a model MP100f sensor (Rotronic, Zurich, Switzerland).

Measurements in California

In California (the data were collected automatically, at 1-hour intervals, using the Campbell Scientific data-logger) at the San Joaquin Valley (latitude 36.6°). Temperature and relative humidity were collected using a HMP35C Vaisala temperature and relative humidity probe (Vaisala Inc., Woburn, MA, USA). Solar radiation was measured by model PSP Eppley Precision Pyranometer (Eppley Laboratory Inc., Newport, RI, USA). Wind speed was measured by a 014A anemometer (Met One Inc., Grant Pass, OR, USA).

Measurements in The Netherlands

Measurements in The Netherlands were collected by a standard meteorological station ('KNMI', The Royal Netherlands Meteorological Institute) at De Kooy (latitude 52.2°), at the extreme north-west part of the country, at the coast. The weather data were collected automatically using standard instruments placed in a 1·5 m height instrument shelter. Wind speed was measured at a height of 10 m by a three-cup anemometer.

THEORY AND RESULTS

Air temperature

The data needed for describing the diurnal air temperature curve were minimum air temperature ($T_{\min(J)}$), maximum air temperature ($T_{\max(J)}$), the minimum air temperature of the next day ($T_{\min(J+1)}$) and day length (DL). Latitude and Julian date were used to compute DL (Spitters *et al.*, 1986). Using these data, the diurnal air temperature can be described by the sine-exponential model (Van Engelen & Geurts, 1983) or by a modification of this method.

Sinusoidal expression during day-time

The general equation for calculating air temperature, T_a during day-time was:

$$T_a = T_{min} + (T_{max} - T_{min})S_{(t)} \tag{1}$$

where T_a is air temperature, T_{min} and T_{max} are the minimum and maximum air temperature respectively. $S_{(t)}$ is a function of time t, ranging between 0 and 1, which we defined as:

$$S_{(t)} = \sin\left(\pi \frac{t - \text{LSH} + \frac{\text{DL}}{2}}{\text{DL} + 2P}\right) \tag{1a}$$

where DL is the day length, LSH is the time of maximum solar height (11·3 h in Israel, 12·1 h in California and 13·5 h in The Netherlands) and P is the delay in the maximum air temperature with respect to the time of maximum solar height. This delay is caused by heat storage in the atmosphere and in the surface layers of the soil. During the rising part of the curve, before the time of maximum temperature, the minimum air temperature of the same day (T_{min}) was used, but after this moment, the minimum air temperature of the next day ($T_{min(J+1)}$) was used.

A flattened shape of the sinusoidal expression

We observed that the time course of the actual temperature data usually deviated from the sinusoidal curve in the following characteristic ways: a faster increase right after sunrise, a plateau-like maximum during several hours in the middle of the day, and a rather fast decrease by sunset. The physical reason of this mid-day flattening is a more efficient mixing of heated air from ground level into the atmospheric boundary layer, driven by the strong lapse temperature gradients generating buoyancy. At the same time, the height of the planetary boundary layer increases (Driedonks, 1981; Holtslag & Nieuwstadt, 1986). Other explanations are a decrease in the radiative flux convergence in the convective boundary layer towards mid-day and an increase in the ratio of the latent to sensible heat flux as the vapour pressure deficit increases. We allowed for this process by correcting the sinusoidal time course.

The simple sinusoidal time course was based on direct proportionality between temperature, and its driving force the solar flux (delayed P hours). If, however, transport of heat to the upper atmosphere is accelerated by increased temperature, a first order approximation is:

$$T_a = T_{min} + \frac{(T_{max} - T_{min}) * S_{(t)} * T_k}{(T_k + T_a - T_{min})} \tag{1b}$$

The parameter T_k specifies the temperature increment at which the transport rate (sensible heat flux) is doubled in comparison with the situation without buoyancy. In equation (1b), T_a appears on both sides of the equation. This equation can be written explicitly as follows (eqn (1c)):

$$T_a = T_{min} - \frac{T_k}{2} + \frac{1}{2}\sqrt{T_k^2 + 4 * AMP * T_k * S_{(t)}} \tag{1c}$$

where AMP is the amplitude of T_{min} and T_{max}, calculated as:

$$AMP = \left(T_{max} - T_{min}\right) * \left(1 + \frac{T_{max} - T_{min}}{T_k}\right) \tag{1d}$$

This expression ensures that the calculated temperature passes through the T_{min} and T_{max} values. We did not intend to develop a theory for the value of T_k. Instead, we determined its value by calibration. For the calibration of the parameter T_k, the duration of the plateau-like part of the diurnal curve was used. We found $T_k = 15$ (C or K degrees) to be appropriate for all three locations.

An exponential expression during the night

Night air temperature was described by an exponentially declining curve in the general form of:

$$T_a = A + B * \exp\left(-\frac{t}{\tau}\right) \tag{2}$$

where τ is a time coefficient. This can be more specifically written as:

$$T_a = \frac{T_{min(J+1)} - T_s * \exp\left(-\frac{\eta}{\tau}\right) + \left(T_s - T_{min(J+1)}\right) * \exp\left(-\frac{t_a - t_s}{\tau}\right)}{1 - \exp\left(-\frac{\eta}{\tau}\right)} \tag{2a}$$

where t_a and t_s are the current time and the time of sunset, respectively, η is the night length ($\eta = 24 - DL$) and τ is a time coefficient. At sunset, T_a starts at the sunset temperature (T_s) and decreases during the night until sunrise, reaching the minimum air temperature of the next day ($T_{min(J+1)}$). T_s connects the day-time and the night time temperature curves. It was calculated with equation (1) using the maximum air temperature (T_{max}) and the minimum air temperature of the next day ($T_{min(J+1)}$). The time of sunset is actually $LSH + DL/2$, so that the time function $S_{(t)s}$ simplifies to:

$$S_{(t)s} = \sin\left(\pi \frac{DL}{DL + 2P}\right) \tag{3}$$

As in the case of T_k, we determined the value of the time coefficient τ, by calibration. We found it to be in the range of 3–5 hours, and we used a mid value of 4 hours in all our calculations.

Measured and calculated air temperatures data for the three sites are presented in Fig. 1a–c. The root mean square error (RMSE) calculated to reflect the overall accuracy of the shape of the simulated curve (Reicosky *et al.*, 1989). The RMSE of the agreement between the measured and the simulated values are given in Table 1 for the T_k and the sine exponential approaches. The T_k model is a refinement of the sine exponential model which only flattens the top of the curve without changing the timing. Input data, the parameter P, the minimum and maximum air temperature of the current day T_{min} and T_{max}, respectively, and the minimum temperature of the next day, $T_{min(J+1)}$, used for the simulation are summarized in Table 2.

Diurnal wind speed

The diurnal wind speed curves appeared to be characterized by the following repetitive pattern: low wind speeds up to the early hours of the morning (T_1), an increase in wind speed from that time up to the late afternoon (T_2), and then a reduction in wind speed to the minimum value in the evening (T_3). The time constants (T_1, T_2 and T_3) used for the calculation of wind speed at the three sites are presented in Table 3. The description of wind speed (W_a) *versus* time (t_a) was done using two sine equations (eqn (4)), differing in time base:

$$W_a = W_{min} + W_{max} * \sin\left(2 * \pi * \frac{t_a - tw_{1,2}}{SF_{1,2}}\right) \tag{4}$$

where $tw_{1,2}$ and $SF_{1,2}$ are time interval factors which depend on the time duration in which wind speed increases or decreases, respectively. It should be noticed that $tw_{1,2}$ and $SF_{1,2}$ are not independent of each other. Their values are related to the time constants as follows (eqns (4a)–(4d)):

$$tw_1 = T_1 \tag{4a}$$

$$tw_2 = 2 * (T_2 - T_3) \tag{4b}$$

$$SF_1 = 4 * (T_2 - T_1) \tag{4c}$$

$$SF_2 = 4 * (T_3 - T_2) \tag{4d}$$

The required inputs are the daily total wind run, TOT_w, the periods in which the wind speed increases from the minimum value and decreases back to this value, and the minimum wind speed value (W_{min}) itself.

On the basis of these quantities, the maximum wind speed, W_{max}, could be calculated (eqn (5)):

$$W_{max} = \frac{(TOT_w - W_{min} * 24 * \frac{3600}{1000}) * 2 * \pi * 1000}{3600 * (SF_1 + SF_2)} \tag{5}$$

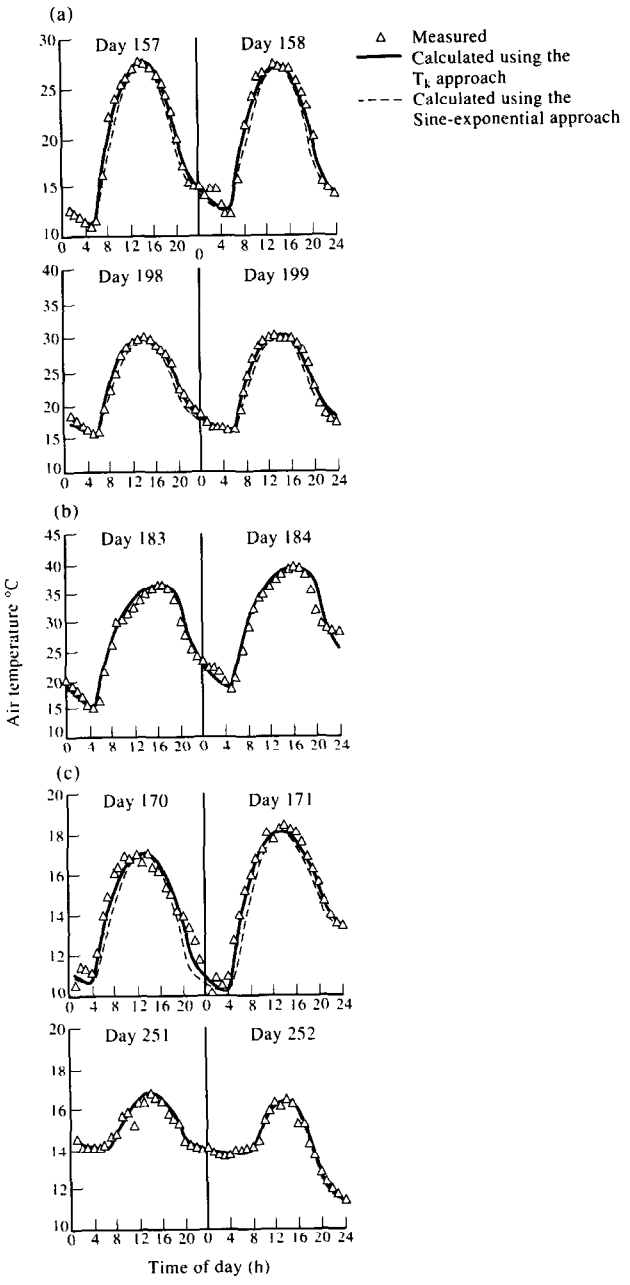

Fig. 1. Calculated diurnal pattern of air temperature using the T_k parameter approach (——), the sine-exponential approach (- - - -) and the measured (△) air temperature at the height of 2 m. (a) Israel, 1987, days 157–158 and 198–199; (b) California, 1991, days 181–182; (c) The Netherlands, 1974, days 170–171 and 251–252. Data for the calculations are summarized in Table 1.

TABLE 1
Summary of the root mean square error[a] (RMSE) of the simulated and measured temperature, wind speed and radiation

Parameter:		*Temperature*		*Wind speed*	*Radiation*
Location	*D.O.Y.*[b]	T_k	*Sine-exp*		
Israel	157	0·66	1·18	1·024	29·34
(Givat-Brener, 1987)	158	0·97	1·41	0·934	17·54
	198	0·47	1·294	0·958	29·11
	199	0·32	1·341	0·938	29·04
California	181	1·55	0·36	1·23	38·95
(San Joaquin Valley, 1991)	182	1·27	0·55	1·34	10·69
The Netherlands	171	0·61	0·96	0·897	41·05
(De Kooy, 1974)	172	0·46	0·84	0·105	41·35
	239			0·899	
	240			1·343	
	251	0·33	0·34		28·87
	252	0·43	0·50		21·59

[a]RMSE was calculated as:

$$\text{RMSE} = \left[\sum_{i=1}^{n}(Do_i - De_i)^{2/}n\right]^{1/2}$$

where Do_i is the observed data, De_i is the estimated data and n is the number of observations (Reicosky *et al.*, 1989).
[b]Day of the year.

TABLE 2
Data used for the calculations of air temperature at three sites

Location	*Latitude*	*D.O.Y.*[a]	T_{max}	T_{min} °C	$T_{min(J+1)}$	*P(h)*
Israel	32·20	157	27·73	10·56	10·69	1·5
(Givaat-Brener, 1987)	32·20	158	27·41	10·69	12·17	1·5
	32·20	198	30·01	15·83	16·32	1·5
	32·20	199	30·70	16·31	15·91	1·5
California	36·60	181	31·16	14·16	14·95	3·5
(San Joaquin Valley, 1991)	36·60	182	36·17	14·95	18·48	3·5
The Netherlands	52·20	171	17·10	10·61	10·24	2·0
(De Kooy, 1974)	52·20	172	18·42	10·24	11·08	2·0
	52·20	251	16·80	14·10	9·10	2·0
	52·20	252	16·40	9·10	2·20	2·0

[a]Day of the year.

TABLE 3
Data used for the calculations of wind speed at three sites

Location	*D.O.Y.*[a]	*Time constants*			*Daily total wind run* ($km\ d^{-1}$)	W_{nytf}
		T_1 *sunrise*	T_2 *hours after noon*	T_3 *sunset*		
Israel	158	1	4	2	76·3	0·0025
(Givaat-Brener, 1987)	159	1	4	2	55·6	0·0025
California (1991)	180	1	3	0	72·6	0·0080
(San Joaquin Valley)	181	1	3	0	69·3	0·0080
The Netherlands	170	1	2	2	64·3	0·0060
(De Kooy, 1974)	171	1	2	2	61·3	0·0060
	238	1	2	2	51·1	0·0060
	239	1	2	2	66·3	0·0060

[a]Day of the year.

where TOT_w, the daily total wind run, is expressed in km d^{-1}, W_{max} and W_{min}, the maximum and minimum wind speeds, in m s^{-1}. For the period between T_3 and T_1 on the next day, wind speed was considered to be at a constant minimum value (W_{min}). The W_{min} was calculated from the ratio between the TOT_w and the wind run sum from T_2 to T_3, divided by the number of hours, W_{nytf} (Table 3).

Measured and calculated wind speed data for the three sites are presented in Fig. 2a–c. The RMSE of the agreement between the measured and the simulated wind speed data are given in Table 1. For intermittently cloudy days the equation reduces the RSME, although the relative improvement is obviously less than on a clear day.

Diurnal global radiation

Diurnal global radiation curve was computed using the measured daily total global radiation (R_g), day length (DL) and the solar elevation ($\sin \beta$), computed from the latitude (L, radians), the solar declination (δ, radians) and time of the day (t_a). To compute the sine of the solar elevation ($\sin \beta$) some intermediate parameters were needed: SD, the seasonal offset of the sine of the solar height:

$$SD = \sin(L) * \sin(\delta) \tag{6}$$

and CD, the amplitude of the sine of the solar height:

$$CD = \cos(L) * \cos(\delta) \tag{7}$$

The sine of the solar elevation, $\sin \beta$, is calculated as:

$$\sin(\beta) = SD + CD * \cos\left(\pi * \frac{t_a - LSH}{12}\right) \tag{8}$$

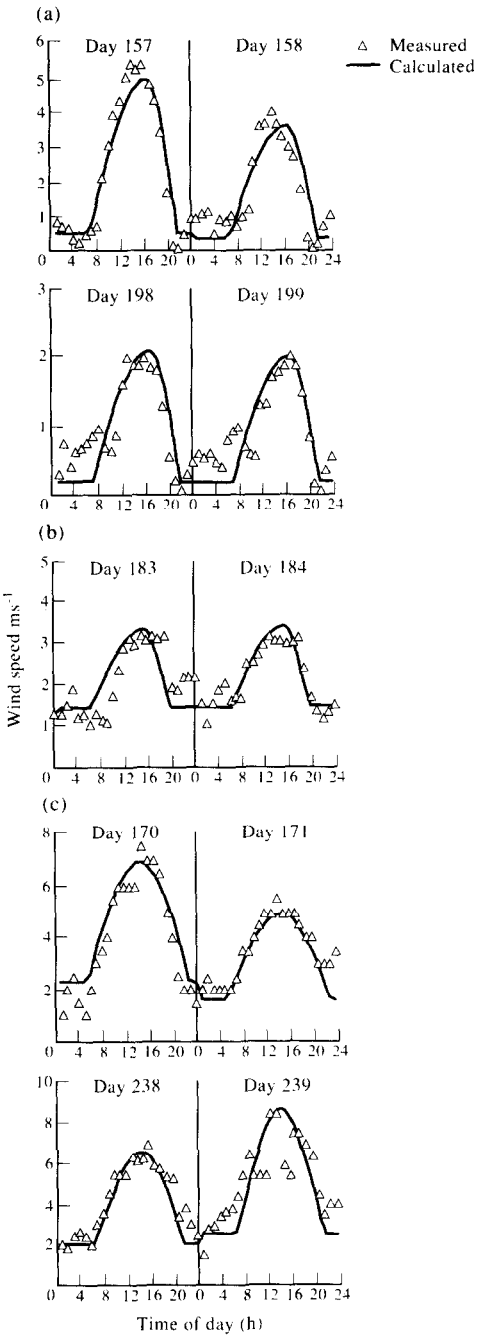

Fig. 2. Calculated (—) and measured (△) wind speed at the height of 2 m. (a) Israel, 1987, days 157–158 and 198–199; (b) California, 1991, days 181–182; (c) The Netherlands, 1974, days 170–171 and 239–240. Data for the calculations are summarized in Table 2.

where t_a is the current time and LSH is the time of maximum solar height (see also eqn (1a)). For the calculation of the diurnal time course of global radiation ($R_{g(a)}$, Fig. 3) a linear increase of the atmospheric transmissivity with the sine of solar height was assumed. Instantaneous radiation ($R_{g(a)}$) is therefore proportional to $\sin\beta*(1 + C*\sin\beta)$ (Spitters *et al.*, 1986).

Its calculation is based on the ratio between the instantaneous value of $\sin\beta*(1 + C*\sin\beta)$ and its integral:

$$R_{g(a)} = R_{g(tot)} * \sin\beta * \frac{1 + C * \sin\beta}{\text{DSBE} * 3600} \tag{9}$$

where DSBE is the daily integral of $\sin\beta*(1 + C*\sin\beta)$ from sunrise to sunset, calculated as:

$$\text{DSBE} = \arccos\left(\frac{-\text{SD}}{\text{CD}}\right) * \frac{24}{\pi} * \left(\text{SD} + C * \text{SD}^2 + \frac{C * \text{CD}^2}{2}\right) + 12 * \text{CD} * (2 + 3 * C * \text{SD}) * \frac{\sqrt{1 - \left(\frac{\text{SD}}{\text{CD}}\right)^2}}{\pi} \tag{10}$$

The parameter C (eqns (9) and (10)) is a fairly constant meteorological variable, equal to about 0·4 (Spitters *et al.*, 1986).

Measured and calculated incoming global radiation for the three sites are presented in Fig. 3a–c. The RMSE of the agreement between the measured and the simulated radiation data are given in Table 1. For intermittently clouded days the equation will reduce the RMSE although the relative improvement is obviously less than on a clear day.

Diurnal relative humidity

Relative humidity (RH) can be derived from the ratio of the actual vapour pressure in the air (VPA) and the saturated vapour pressure (e_s):

$$\text{RH}(\%) = 100 * \frac{\text{VPA}}{e_s} \tag{11}$$

ES is a function of actual air temperature (T_a), (Goudriaan, 1977):

$$e_s = 6{\cdot}107 * \exp\frac{T_a * 17{\cdot}4}{239 + T_a} \tag{12}$$

The actual VPA is similarly related to $T_{d(cal)}$, the calculated dew point temperature in °C.

$$\text{VPA} = 6{\cdot}107 * \exp\frac{T_{d(cal)} * 17{\cdot}4}{239 + T_{d(cal)}} \tag{13}$$

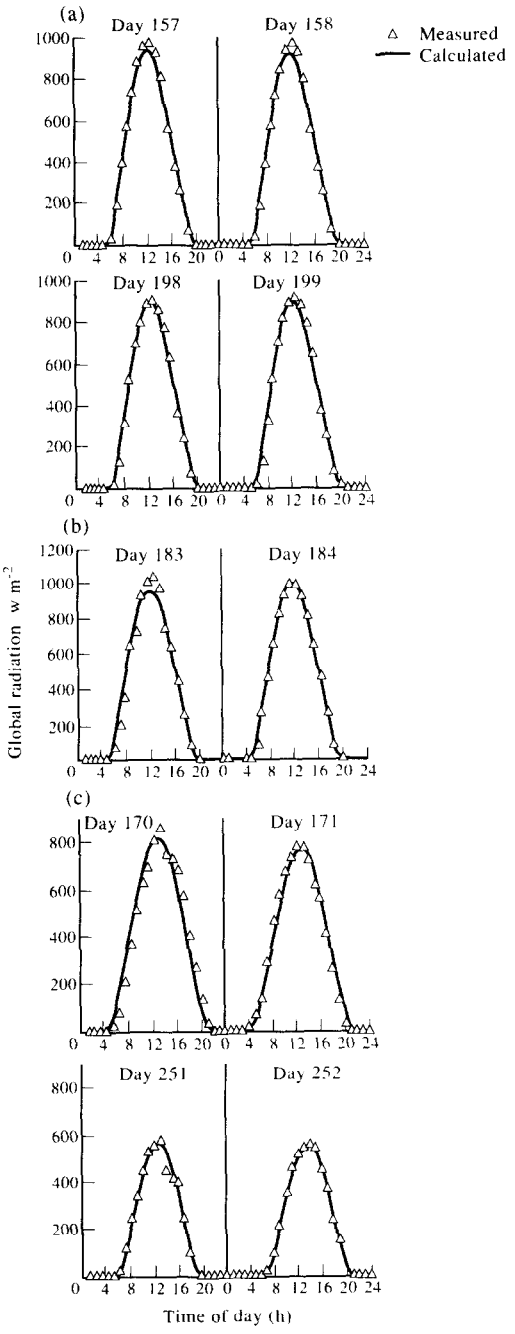

Fig. 3. Calculated (—) and measured (△) incoming global radiation. (a) Israel, 1987, days 157–158 and 198–199; (b) California, 1991, days 181–182; (c) The Netherlands, 1974, days 170–171 and 251–252.

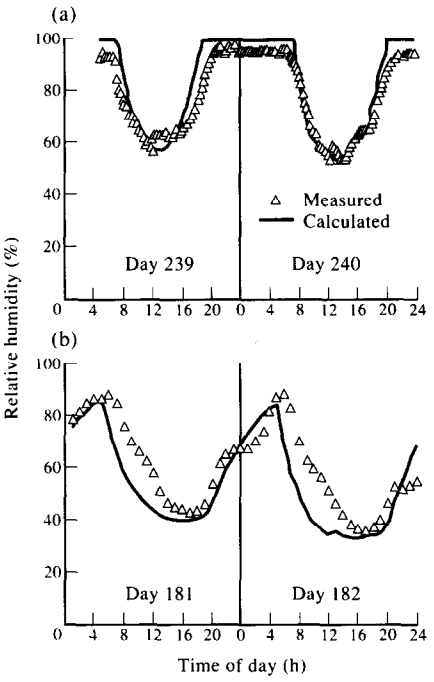

Fig. 4. Calculated (—) and measured (△) relative humidity at the height of 2 m. (a) Israel, 1987, days 239–240; (b) California, 1991, days 181–182. The calculations of relative humidity were based on the dew point temperature (T_d) approach (for details see Theory and results).

The correct estimation of $T_{d(cal)}$ is therefore crucial for obtaining good estimates of RH. This is strongly dependent on site characteristics. We have found that there is a site-specific value for the maximum dew point temperature $T_{d(max)}$. When air temperature is less than $T_{d(max)}$ (usually from the afternoon until the next morning) $T_{d(cal)}$ was equal to air temperature and the air was saturated. When air temperature was higher than $T_{d(max)}$, $T_{d(cal)}$ was considered to be equal to $T_{d(max)}$:

$$T_{d(cal)} = \min(T_d, T_{d(max)}) \tag{14}$$

$T_{d(max)}$ was found to be about 24°C during the summer in the coastal plain of Israel. In the San Joaquin Valley of California, however, we have found that the value of $T_{d(max)}$ was 11°C for days with a maximum temperature of 24°C or lower, 15°C for days with a maximum of 40°C or higher, and a linear interpolation was used when the maximum was in the range of 24–40°C.

Measured and calculated relative humidity data for 2 days in 1987 in Israel and for 2 days in 1991 in California are presented in Fig. 4. No data were available for The Netherlands.

CONCLUSIONS AND DISCUSSION

We have found that the description of the diurnal curve of air temperature by the sine-exponential model (Van Engelen & Geurts, 1983) was not sufficiently accurate in most cases. Maximum temperature is usually later than solar noon. Air temperature also remains more constant at the middle of the day than described by the sine-exponential model. Three site-specific parameters are required for the description of diurnal air temperature. The parameter P (eqn (1a)) expresses the time lag of the maximum temperature after solar noon. The parameter T_k (eqn (1b)) allows for the effect of buoyancy. The parameter T_k only flattens the top and does not move the timing of the diurnal curve. These two parameters significantly improved the calculation of temperature during day-time. For the exponential segment of the curve a third parameter is needed — the time coefficient τ.

All these three parameters may have different values at different geographical regions, or perhaps they may also vary between seasons during the year. The main requirement for using this approach is therefore to determine the values of these parameters. We have found the values of T_k and τ to be the same for all the three locations we have examined. The value of P, which was found to vary from one location to the other, can easily be determined for each site.

This method worked very well for the three locations (Fig. 1a–c), during most of the summer season. Comparison of the RMSE (Table 1) of the estimated air temperatures by the T_k and the sine-exponential approaches shows an advantage to the T_k approach: the closer the estimated temperatures are to the observed temperature, the smaller the RMSE. It should be noted, however, that when a weather front passes through during the day, no regular pattern can describe the diurnal changes in temperature or in other weather variables.

Several methods exist for describing diurnal wind speed curves (Peterson & Parton, 1983). Investigating the wind speed patterns at the three sites (Israel, California and The Netherlands), we have found that wind speed during the night was very low and nearly constant most of the time (Fig. 2a–c). We have also found that the increase and decrease of wind speed during day-time could be described by two sine curves (Fig. 2, eqn (4)). The minimum wind speed values may vary from one location to another, depending on the topographical characteristics of the location and the distance from the sea. Furthermore, the period of time during the day in which the wind speed is at its minimum value may change as a result of the same reasons.

Although there is naturally a considerable variation in wind speed during the season, we have found this method to be convenient and useful.

The following site-specific parameters (Table 3) are needed for this method: the time in which the wind speed increases from the minimum value (after sunrise, T_1); the time of maximum wind speed (after solar noon, T_2); the time it decreases back to the minimum (after sunset, T_3); and the ratio between the minimum (night time) wind speed and the total daily wind run, W_{nytf}. Once the definition of those parameters was set, it can be used for the calculation of wind speed for a long period of time during the year. It should be noted, however, that wind speed is a very unstable climatic characteristic, and its pattern may often be unpredictable.

In the case of the diurnal trend of the global radiation ($R_{g(a)}$, Fig. 3, eqn (9)) only one parameter, C, is required, which we have found to be constant at all the three locations. The same method may also be used for computing the photosynthetically active radiation (PAR, 400–700 nm) which is needed for the calculation of the photosynthetic rate (Spitters *et al.*, 1986).

Calculation of relative humidity is based on the dew point temperature (eqns (11)–(14)). Because dew point temperature data are not available in many cases, we estimated it from temperature data. This is of course site-specific to a large extent. The method involves the definition of a maximum dew point temperature. This may be fairly constant during the whole season (as in the coastal plain of Israel during the summer), or vary during the season. It was found to be strongly dependent on the daily maximum temperature in the San Joaquin Valley of California. The method for calculating the diurnal course of the relative humidity is thus strongly affected by site characteristics. Kimball & Bellamy (1986) reported that daily fluctuations of vapour pressure are usually very small. Daily average data of vapour pressure (or dew point temperature) would certainly increase the accuracy of the generated relative humidity curve.

It is obvious that the methods presented here cannot be considered as site- or season-independent. It is also expected that the diurnal pattern of weather data may sometimes be of a random nature. In particular, wind speed patterns may vary widely from location to location or even from day to day. The purpose of this study was to characterize the diurnal curves by simple methods, and by as few parameters as possible. Considering the constraints of site dependency, our methods provide good estimation.

ACKNOWLEDGEMENT

The authors wish to express their thanks to The Royal Netherlands Meteorological Institute (KNMI) for the meteorological data used in this manuscript, which were obtained from De Kooy.

REFERENCES

Bernhardt, J. L. & Shepard, M. (1978). Validation of physiological day equation: development of the Mexican bean beetle on snap beans and soybeans. *Environ. Entomol.*, **7,** 131–5.

Björkman, O. (1979). The response of photosynthesis to temperature. In *Plants and Their Atmospheric Environments*, eds J. Grace, E. D. Ford & P. G. Jarvis. Blackwell Scientific Publishers, Boston.

Driedonks, A. G. M. (1981). Dynamics of the well-mixed atmospheric boundary layer. *Scientific Report 81–2*, Royal Netherlands Meteorological Institute, De Bilt.

Floyd, R. B. & Braddock, R. D. (1984). A simple method for fitting average diurnal temperature curves. *Agric. For. Meteorol.*, **38,** 217–29.

Geng, S., Penning de Vries, F. W. T. & Supit, I. (1985). Analysis and simulation of weather variables. II. Temperature and solar radiation. *Simulation Report CABO-TT No. 5*. Wageningen, The Netherlands.

Goudriaan, J. (1977). *Crop Micrometeorology: A Simulation Study*. Pudoc, Wageningen.

Holtslag, A. A. M. & Nieuwstadt, F. T. M. (1986). Scaling the atmospheric boundary layer. *Boundary-layer Meteorol.*, **36,** 201–9.

Kimball, B. A. & Bellamy, L. A. (1986). Generation of diurnal solar radiation, temperature and humidity patterns. *Energy Agric.*, **5,** 185–97.

Penman, H. L. (1948). Natural evaporation from open water, bare soil and grass. *Proc. R. Soc.*, **A193,** 120–45.

Peterson, T. C. & Parton, W. J. (1983). Diurnal variations of wind speeds at the shortgrass prairie site — a model. *Agric. Meteorol.*, **28,** 365–74.

Reicosky, L. J., Winkelman, L. J., Baker, J. M. & Baker, D. G. (1989). Accuracy of hourly air temperatures calculated from daily minima and maxima. *Agric. For. Meteorol.*, **46,** 193–209.

Richardson, C. W. (1981). Stochastic simulation of daily precipitation, temperature, and solar radiation. *Water Resource Res.*, **17,** 182–90.

Richardson, C. W. (1982). Dependence structure of daily temperature and solar radiation. *Trans. ASAE*, **253,** 735–9.

Spitters, C. J. T., Toussaint, H. A. J. M. & Goudriaan, J. (1986). Separating the diffuse and direct component of global radiation and its implications for modeling canopy photosynthesis. Part I. Components of incoming radiation. *Agric. For. Meteorol.*, **38,** 217–29.

Van Engelen, A. F. V. & Geurts, H. A. M. (1983). Een rekenmodel dat het verloop van de temperatuur over een etmaal berekent uit drie termijnmetingen van de temperatuur. *K.N.M.I. Report No. 165-3*, De Bilt, The Netherlands. (in Dutch).

Wang, J. Y. (1960). A critique of the heat unit approach to plant response studies. *Ecology*, **41,** 785–90.